ELSEVIER

Journal of Chromatography B, 782 (2002) 343–351

JOURNAL OF CHROMATOGRAPHY B

www.elsevier.com/locate/chromb

Development of high-throughput liquid chromatography injected ion mobility quadrupole time-of-flight techniques for analysis of complex peptide mixtures

Young Jin Lee[a], Cherokee S. Hoaglund-Hyzera[a,1], Catherine A. Srebalus Barnes[a,1], Amy E. Hilderbrand[a], Stephen J. Valentine[b], David E. Clemmer[a,*]

[a]*Department of Chemistry, Indiana University, Bloomington, IN 47405, USA*
[b]*Beyond Genomics, 40 Bear Hill Road, Waltham, MA 02451, USA*

Abstract

The development of a multidimensional approach involving high-performance liquid chromatography (LC), ion mobility spectrometry (IMS) and tandem mass spectrometry is described for the analysis of complex peptide mixtures. In this approach, peptides are separated based on differences in their LC retention times and mobilities (as ions drift through He) prior to being introduced into a quadrupole/octopole/time-of-flight mass spectrometer. The initial LC separation and IMS dispersion of ions is used to label ions for subsequent fragmentation studies that are carried out for mixtures of ions. The approach is demonstrated by examining a mixture of peptides generated from tryptic digestion of 18 commercially available proteins. Current limitations of this initial study and potential advantages of the experimental approach are discussed.

Keywords: Ion mobility spectrometry; Quadrupole time-of-flight mass spectrometry; Proteomics; Peptide mixtures

1. Introduction

The recent development of gentle sources for mass spectrometry (MS) has revolutionized the analysis of proteins [1,2]. It is now routine to determine accurate molecular masses of proteins [3,4], and methods for obtaining information about sequence [5], sites of post-translational modification [6], and patterns of regulation [7] are proliferating. A number of strategies have been used to address the complex mixtures of proteins that are encountered in the emerging field of proteomics [8]. Our group has become interested in hyphenated techniques that involve multiple separation dimensions combined with MS. In particular, we have coupled a gas-phase separation, ion mobility spectrometry (IMS) [9–11], with time-of-flight (TOF) MS for the analysis of complex protein [12] and peptide mixtures [12–16] (as well as mixtures of other molecules [17,18]). The approach has a number of attractive features. For example, because the mobility separation occurs after the ionization step, it is often possible to delineate chemical noise from signals of interest [19]. Additionally, the mobilities of ions through gases are high—allowing ions to be dispersed throughout the drift tube on ms timescales. This dispersion is the basis of a method for carrying

*Corresponding author. Tel.: +1-812-855-8259; fax: +1-812-855-8300.
E-mail address: clemmer@indiana.edu (D.E. Clemmer).
[1]Current address: Eli Lilly & Co., Indianapolis, IN 46285, USA.

1570-0232/02/$ – see front matter
PII: S1570-0232(02)00569-X

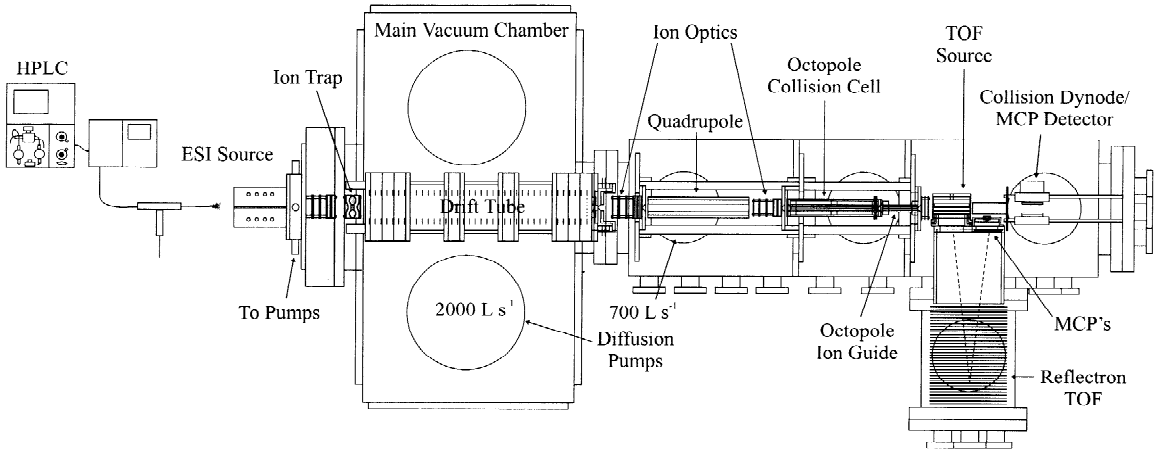

Fig. 1. Schematic diagram of the experimental apparatus. The main features of this instrument include a HPLC system coupled to an atmospheric pressure ESI source. Ions that enter the instrument are accumulated in an ion trap and then injected into the drift tube. Ions exit the drift tube and are focused into a tandem mass spectrometer (a Q-TOF geometry instrument). See text and Ref. [22] for details.

out fragmentation studies for mixtures of ions in a parallel fashion in which fragments are effectively ''labeled'' according to the drift time of the corresponding parents [20–22]. Finally, the approach is rapid, making it suitable for high-throughput analyses. The ms timescale associated with the IMS-TOF measurement allows the two-dimensional analysis to be coupled with additional dimensions of condensed-phase separation approaches, such as reversed-phase high-performance liquid chromatography (HPLC) [23–25][2].

In this paper initial attempts to couple the parallel mobility-based fragmentation technique with an additional LC separation are described. The value of this work is in the fact that it is important step for the possible use of this technique in the real proteomics application. We demonstrate this approach by examining a mixture of peptides that arises from tryptic digestion of 18 commercially available proteins. Although the methods and instrumentation are still under development, the ability to generate fragments from complex mixtures (without initial mass selection) is clearly demonstrated. A brief discussion of current limitations of this initial study as well as some potential advantages of the overall strategy is given.

2. Experimental

2.1. General overview of the HPLC–IMS-TOF approach

Detailed discussions of ion mobility techniques have been given previously [26]. Only a brief description is given here. Fig. 1 shows a schematic diagram of the laboratory-built ion trap and injected-ion drift tube instrument coupled to a Waters 600 series HPLC system. A detailed description of the capabilities associated with the injected-ion drift tube instrument has been presented elsewhere [22] and only a brief description is given here. Peptides from the HPLC system are ionized by continuously electrospraying effluents directly into the source of the IMS-Q-TOF instrument. The continuous beam of ions that enters the instrument is accumulated in an ion trap (Model C-1251; R.M. Jordan, Grass Valley, CA, USA) and ion packets are periodically injected into the drift tube (This ion accumulation approach is described in detail in Ref. [27]). The drift tube is operated at pressures of ~2 to 3 Torr of 300 K

[2]Recently, Hill and co-workers have developed a related approach that couples LC and IMS with quadrupole MS detection. See Ref. [25].

helium buffer gas (1 Torr=133.322 Pa). Ions drift through the gas under the influence of a weak electric field (typically 5 to 12 V cm^{-1}) that is created by a series of 40 equally-spaced BeCu electrodes inside the tube, and separate according to differences in their mobilities through the gas. For a given charge state, compact ions have higher mobilities than elongated ions [26,28]. Under these conditions, the resolving power of the drift tube [$t_D/\Delta t_D$, where t_D is the measured drift time and Δt_D corresponds to the full width at half maximum (FWHM) of the peak] is ~20 for most singly-charged ions and can be >40 for multiply charged ions [22].

Ions exit the drift tube through a differentially pumped orifice-skimmer cone region that has been described previously [21]. The skimmer cone is designed to focus mobility-separated ions (radially diffuse clouds by the end of the drift tube) through a small aperture at the back of the drift tube [21] and can also be used to generate fragment ions (a feature that is not employed in the present study). Upon exiting the skimmer-cone region, ions are focused into a quadrupole mass filter that can be used to select a specific m/z ion, or set to transmit all ions. Here, we operate the quadrupole in the transmission mode.

Ions are collisionally activated (and dissociated) by accelerating them through a 20 to 40 V potential before injection into an octopole collision cell. The collision cell is filled with ~0.18 to 0.20 mTorr of Ar gas. The target gas pressure is kept low so that there are no significant time delays associated with transmission of ions through this region [29]. Upon exiting the collision cell, ions are focused into the source region of an orthogonal geometry TOF mass spectrometer. Typical resolving powers of the mass spectrometer (defined here as $t_F/2\Delta t_F$, where t_F is the measured flight time and Δt_F is taken as FWHM of the peak) range from ~800 to 1500. The instrument can be operated in a number of modes to obtain ion mobility distributions, time-of-flight mass spectra, collision induced dissociation patterns, or combinations of these. The electronics and data acquisition systems were designed and constructed in the laboratory and have been described previously [30].

An important consideration in the present multi-dimensional strategies is associated with differences in the timescales of various measurements. Large differences in ion transit times through the drift tube (~1 to 6 ms) and the evacuated flight tube of the mass spectrometer (~10 to 35 μs), allow flight time distributions to be recorded within individual drift time windows. We refer to this as a nested drift (flight) time measurement; the positions of individual peaks are delineated as $t_D(t_F)$ and unless otherwise noted, are given in units of ms(μs). In some cases, we convert values of t_F to m/z and present the positions of peaks in units of ms(Da).

The ms timescale associated with nested $t_D(t_F)$ measurements is short, allowing this approach to be coupled with slower LC separations. To define the position of a peak in three dimensions, we provide the retention time followed by the drift(flight) time notation, $t_R[t_D(t_F)]$. Unless otherwise stated, the retention time (t_R) is reported in minutes and is taken as the average time recorded for given retention time windows. In the data presented below, the LC separation is acquired by recording $t_D(t_F)$ datasets for 30 s increments. A dead time of ~4 s between each $t_D(t_F)$ frame arises while datasets are saved.

2.2. Sample preparation

The following proteins were obtained from Sigma (purities of ≥90%, unless otherwise noted) and used without further purification: albumin (bovine, dog, pig, and sheep); aldolase (rabbit muscle); β-casein (bovine); β-lactoglobulin (bovine); carbonic anhydrase (bovine); cytochrome *c* (horse); enolase (yeast, ~70%), hemoglobin (human, pig and rabbit); glucose oxidase (*Aspergillus niger*, ~80%); insulin (bovine); lysozyme (chicken egg white); myoglobin (horse); and ubiquitin (bovine). Mixtures of tryptic digest peptides are prepared by combining 1.0 ml of ~20 mg ml^{-1} solution of each protein in 0.2 *M* ammonium hydrogencarbonate (EM Science, Gibbstown, NJ, USA) with 150 μl of 2.0 mg ml^{-1} trypsin (bovine pancrease, TPCK treated; Sigma, St. Louis, MO, USA) solution in 0.2 *M* ammonium hydrogencarbonate and incubating for 20 h at 37 °C. The trypsin is filtered from the digest using a microconcentrator (microcon 10; Amicon, Bedford, MA, USA) and the peptides that remain are lyophilized.

Prior to recording $t_R[t_D(t_F)]$ datasets for the com-

plete mixture, $t_D(t_F)$ data were acquired for tryptic peptide mixtures of each protein. Over the m/z range of our study (100 to 1500) it is possible to assign 470 peptides to expected tryptic fragments (including some missed cleavages). This value is near a value of 512 tryptic digest peptide sequences that we calculate should be present over this mass range (assuming complete digestion).

2.3. HPLC separation

Reversed-phase HPLC separation of the peptide mixtures is performed using a Waters 600 series HPLC system and a C_{18} column (Xterra MS C_{18}, 3.5 μm, 4.6×150 mm; Waters, Milford, MA, USA). A solvent mixture of water (0.1% formic acid)–acetonitrile (0.1% formic acid, ACN) is used as the chromatographic mobile phase with the following gradient sequence: 0 to 120 min (10 to 45%, ACN), 120 to 125 min (45 to 100%, ACN), 125 to 130 min (100%, ACN). The chromatogram is recorded using a detector wavelength of 214 nm, a mobile phase flow-rate of 0.25 ml min^{-1}, and a column temperature of 35 °C. HPLC effluents are split at a ratio of 1:200 to give the appropriate flow-rate for electrospray. A total concentration of 18 mg ml^{-1} of the mixture sample was injected into the LC system through a 200-μl loop and 18 μg of total mixture sample is supposed to be introduced into the IMS instrument after the 1:200 split.

3. Results and discussion

3.1. Overview

In the discussion that follows, we present an overview of results obtained for more than 220 different $t_D(t_F)$ datasets that are acquired for each LC separation. The data that are shown come from two types of experiments. The first experiment involves a two-dimensional separation (LC–IMS) followed by TOF-MS analysis. We refer to this as a parent ion analysis. The second experiment is identical to the first except that a collision gas is added to the octopole collision cell in order to generate fragment ions, and ion focusing elements are adjusted to collect fragments. We refer to this as a fragment ion analysis.

3.2. Analysis of several peaks from parent and fragmentation $t_R[t_D(t_F)]$ datasets

Fig. 2 shows a two-dimensional $t_R[t_D]$ contour plot of the intensity of peaks across the LC and IMS dimensions in the $t_R[t_D(t_F)]$ dataset. These data correspond to a parent ion spectrum (data recorded without a collision gas). Ion intensities are obtained by summing signal across all flight time bins. The complete dataset is made up of 223 different $t_D(t_F)$ distributions; over the range of elution times that are shown (10 to 140 min) ion drift times range from ~1.5 to 5.5 ms. A preliminary analysis of these data indicates that more than 400 peaks are at least partially resolved across these two dimensions. We note that the source conditions that we have used favor $[M+2H]^{2+}$ and higher charge states (primarily having drift times from ~2.0 to 3.5 ms); under other conditions we observe many more peaks associated with $[M+H]^{+}$ ions which have longer drift times (~2.5 to 7.0 ms under the conditions employed over a mass range of ~300 to 1500 Da).

Additional information that can help assign features to specific peptides comes from considering the data in the TOF dimension. An example of a typical mass spectrum for one of the spots observed in the two-dimensional $t_R[t_D]$ plot is shown in Fig. 3. This spectrum is obtained from the intensities associated with the intersection at $t_R[t_D]=36[2.4]$ and is shown as intensity as a function of the t_F dimension. Some progress in assigning peaks in the $t_R[t_D]$ plot to specific sequences is made by comparing experimental m/z values (determined from measurements of t_F) to values that are calculated for $[M+nH]^{n+}$ (where $n=1$ to 3) forms of peptides that are expected to be present. Because we have prepared the mixture from commercially available proteins and have measured m/z values and mobilities for individual protein digests, it is relatively straightforward to assign many peaks that are observed in the $t_R[t_D]$ plot (Fig. 2) to peptides that are expected to be present in the mixture[3]. For the example parent ion mass spectrum shown in Fig. 3, we observe a large peak at m/z 384.3 and a smaller peak at m/z 378.4. Although a

[3]Tryptic digest peptide lists were made using the web database (http://www.expasy.org) with a possible number of two missed cleavages.

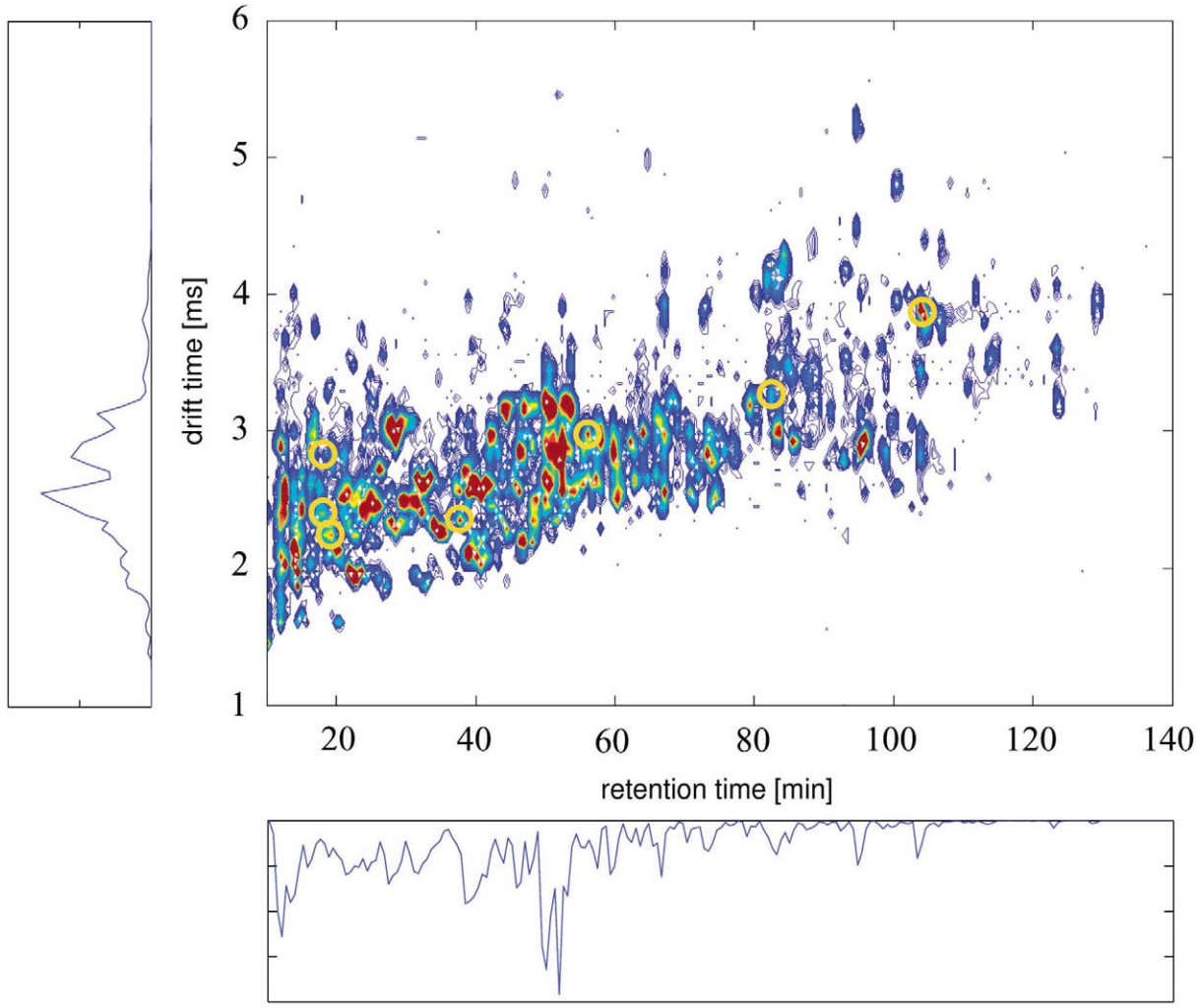

Fig. 2. Two dimensional contour plot of the parent ion retention[drift] time ($t_R[t_D]$) distribution. Ion intensities are shown on a false color scale where red indicates the most intense features. Ion intensities are obtained by integrating ion counts across all flight times at each drift time in 223 nested $t_D(t_F)$ datasets. See text for details. Some peaks are encircled in yellow. These are randomly chosen areas of the spectrum that are discussed in the text. Parent ion and fragment ion mass spectra for the feature at $t_R[t_D]$=36[2.4] are shown in Fig. 3. The total ion drift time distribution is shown on the left. This distribution is obtained by integrating the ion counts for all retention times at each drift time in the two-dimensional $t_R[t_D]$ dataset. The ion chromatogram on the bottom is obtained by integrating the ion counts for all drift times at each retention time in the $t_R[t_D]$ dataset.

TOF resolving power of $m/\Delta m > 1000$ has been determined from some of the peaks in this dataset, isotopic structure for the peak at m/z 384.3 is not resolved; this indicates that the spacing between these features is below the 0.5 spacing for $[M+2H]^{2+}$ ions. This peak (and also the smaller peak at 378.4) must correspond to $n=3$ (or higher) charge state ions. From our list of calculated m/z values for peptides that are expected to be present, we find that three sequences are in reasonable agreement with the m/z 384.3 experimental value: $[VVAGVANALAHK+3H]^{3+}$ from hemoglobin (human, pig and rat), having m/z_{calc} 383.90 for the monoisotopic ion; $[DGNKSEWMGK+3H]^{3+}$ from enolase, having m/z_{calc} 384.51; and, $[ALKALPMHIR+3H]^{3+}$ from β-lactoglobulin, having m/z_{calc} 383.93. While we have made progress in assigning this peak based on the parent ion m/z

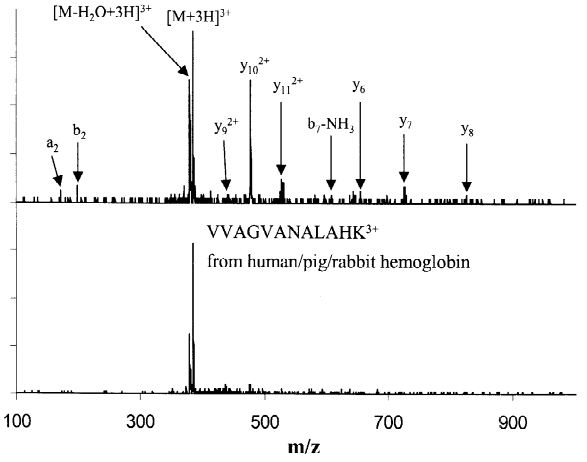

Fig. 3. Parent (bottom) and fragment (top) ion mass spectra for a single peptide ion with $t_R[t_D]=36[2.4]$. The mass spectra are obtained from a slice centered at $t_D=2.4$ ms across the $t_D(t_F)$ dataset obtained at $t_R=36$ min. See text for a discussion.

determination, this spectrum alone is not sufficient to make an unambiguous assignment.

Seven additional examples of experimental $t_R[t_D(t_F)]$ values (and possible assignments) are listed in Table 1 for randomly chosen peaks across the parent ion dataset. The $t_R[t_D]$ positions are indicated in Fig. 2 by circles. In each of these cases, the current accuracy of the m/z measurement is insufficient for an unambiguous assignment. In these cases, additional information obtained from fragment ion data can often eliminate ambiguities.

Fig. 3 also includes a plot of the TOF dimension obtained at $t_R[t_D]=36[2.4]$ in the fragment ion spectrum recorded immediately after the parent ion dataset. Two experimental changes between these scans were made: (1) the octopole collision cell was filled with Ar; and, (2) other focusing elements were optimized for generating and collecting fragment ions. Under these conditions, values of t_R and t_D for most ions are nearly identical to those recorded in the earlier parent ion experiment. However, the mass spectra are clearly different. The example shown in Fig. 3 illustrates that a substantial fraction of the m/z 384.3 parent ions have dissociated. From a comparison of m/z values for fragment ions with fragment masses that are expected for the VVAGVANALAHK, DGNKSEWMGK, and ALKALPMHIR possible parent ions (using the Protein Prospector code) [31], the most plausible assignment of the 384.3 ion is as $[VVAGVANALAHK+3H]^{3+}$. Especially important in this assignment is the observation of several b and y series fragments. We also note that the relative intensity of the peak at 378.4 increases in the fragment ion scan. We tentatively assign this peak to the $[M\text{-}H_2O+3H]^{3+}$. Apparently a small amount of collisional activation occurs after the mobility separation even when no gas is added to the octopole collision cell (in the parent ion spectrum). It is possible that this occurs in the orifice skimmer-cone region of the drift tube (even at low extraction potentials).

Several additional examples, in which the fragment ion spectrum is useful in confirming (or defining) a sequence are provided in Table 1. Three different parent ions at $t_R[t_D\ (m/z)]=18[2.2\ (380.2)]$, 18[2.4 (391.0)], and 19[2.8 (651.0)] have nearly identical retention times but are resolved in the ion mobility dimension. The fragment information recorded in parallel allows assignments for each of these peaks to be made (Table 1). Information about other peaks across the two dimensional separation is also included in Table 1.

4. Summary and conclusion

An initial investigation of a multidimensional approach for analyzing large mixtures of peptides that couples LC and IMS separations with MS and MS–MS has been presented. The approach was illustrated by examining a mixture of tryptic peptides obtained from digestion of 18 proteins. More than 400 peaks associated with peptide ions are resolved across the two-dimensional $t_R[t_D]$ separation. Although not stressed in the present work, previous work has shown that the ion mobility measurement is highly reproducible [9–11] and thus, can be used as an additional constraint for assigning peptide sequence.

An important aspect of the current approach is the ability to utilize collision induced dissociation patterns as a means of identifying large mixtures of peptides. In the current approach, ions are dispersed in a drift tube (rather than mass-selected in the quadrupole) prior to collisional activation. With this approach, the fragment ions that are formed are

Table 1
Summary of several assigned parents and fragments

Observed parent		Possible parent ion[b]		Assigned fragments[c]
$t_R[t_D\ (m/z)]$[a]	m/z_{cal}	Sequence	Protein	
18[2.2 (380.2)]	380.23	IVTDLAK^{2+}	Albumin(p)	y_6, y_5, a_4, TDLA-H20, TDLA-28, a_3, b_2, a_2, y_1
18[2.4 (391.0)]	390.75	VLPVPQK^{2+}	β-Caesin	y_6-NH_3, b_6-NH_3, y_5, y_4, a_4, b_3, y_5^{+2}, b_2, a_2
19[2.8 (651.0)]	650.87	ALQASALKAWGGK^{2+}	Aldolase	b_8, y_6, b_{10}^{2+}, a_6, a_{10}^{2+}, y_{10}^{2+}, b_5, y_9^{2+}, y_4, y_8^{2+}, a_9^{2+}, y_3, a_3
	651.33	LEQWAEEAVAR^{2+}	Glucose Ox.	
	651.31	MTTSDGSQYLAK^{2+}	Carbonic Anh.	
	650.82	TVMGDFGAFVEK^{2+}	Albumin(d)	
	650.36	HPDYSVSLLLR^{2+}	Albumin(p)	
36[2.4 (384.3)]	383.90	VVAGVANALAHK^{3+}	Hemoglubin(h/p/r)	y_8, y_7, y_6, b_7-NH_3, y_{11}^{2+}, y_{10}^{2+}, y_9^{2+}, $[M\text{-}H_2O+3H]^{3+}$, b_2, a_2
	384.51	DGNKSEWMGK^{3+}	Enolase	
	383.90	ALKALPMHIR^{3+}	β-Lactoglobulin	
56[3.0 (534.1)]	533.30	VLVLDTDYK^{2+}	β-Lactoglobulin	y_7, y_6, y_5, *b_5*, y_8^{2+}, *y_8-NH_3^{2+}*, y_9-H_2O^{2+}
	534.31	ESTLHLVLR^{2+}	Ubiquitin	
	533.63	FLANVSTVLTSKYR^{3+}	Hemoglobin(p/r)	
	533.60	KTGQAPGFTYTDANK^{3+}	Cytochrome *c*	
56[3.0 (627.4)]	626.86	FLASVSTVLTSK^{2+}	Hemoglobin(h)	y_6, *y_5, a_6, 572.5, y_5, b_5, a_5, y_{10}-H_2O^{2+}, VSTVL-28*
	628.88	VLASSARQRLR^{2+}	Albumin(b/s)	
	626.83	FPKADFAEISK^{2+}	Albumin(d)	
	627.96	GVFAECCQAADKAACLGPK^{3+}	Albumin(d)	
	627.71	GVTKAVSNVNSIIGPALIK^{3+}	Enolase	
82[3.3 (772.3)]	771.76	VYVEELKPTPEGDLEILLQK^{3+}	β-Lactoglobulin	b_{12}-NH_3, YVEELKPTPE-NH_3, y_{19}^{2+}, a_9, a_7, y_{14}^{2+}, b_{14}^{2+}, y_{14}-H_2O^{2+} y_6, b_{13}^{2+}, a_{11}^{2+}, y_{11}^{2+}
	772.92	GACLLPKIDAMREK^{2+}	Albumin(s)	
	772.69	YNGVFQECCQAEDKGACLLPK^{3+}	Albumin(b/s)	
104[3.99 (1026.9)]	1027.22	LLGNVLVCVLAHHFGKEFTPPV QAAYQK^{3+}	Hemoglobin(h)	a_{22}^{2+}, y_{10}, b_{11}, b_{11}-NH_3, a_{11}, NVLVCVLAHH-28, y_9-NH_3, b_9, a_9, b_8, a_8, b_7, VLAHHF, a_{18}^{3+}
	1027.58	IVAPGKGILAADESTGSIAKR^{2+}	Aldolase	
	1026.54	HGEYGFQNALIVRYTRK^{2+}	Albumin(s)	
	1026.50	LSELHCDKLHVDPENFR^{2+}	Hemoglobin(r)	
	1026.48	LSELHCDQLHVDPENFR^{2+}	Hemoglobin(p)	
	1026.07	QSPVNIVTAKTQLDPNLGR^{3+}	Carbonic anhydrase	
	1027.22	SILEPLGIDTVVDLPVGLNLQDQ TTATVR^{3+}	Glucose oxidase	

[a] Parent ion experimental retention time, drift time, and m/z in units of min, ms, and Da, respectively.

[b] Tryptic peptide ion from a list of expected digest peptides (Ref [31].) with calculated m/z within a ±0.1% window of the observed value. For the given data, the ion mobility distributions and isotropic mass distributions allow the exclusion of singly-charged peptide ions.

[c] Fragment assignments are given only for the most plausible peptide sequences determined by the comparison of fragment passes between observed and estimated (Ref [32].). In cases where multiple fragment assignments are possible, only the m/z is given. For the case of $t_R[t_D]$=56[3.0], two parent ions are observed and assignments are shown in italics if they cannot be unabiguously ascribed to one parent.

coincident with their antecedent parent ions. This coincidence can be used as a label for fragments that are associated with the same parents [20]. We have already demonstrated that it is possible to examine fragmentation patterns for dozens of parent ions in parallel [22]. The initial LC separation extends this approach to significantly more complex mixtures; in effect, the $t_R[t_D]$ values for a specific ion can be thought of as a two-dimensional label for MS–MS studies.

It is worthwhile to note here that the injected ion mobility instrument used in this study has much better sensitivity than the high-resolution ion mobility instrument we used in the previous work [23,24] so we could have enough sensitivity to get CID dataset in a single LC run. From a preliminary

analysis of the data presented here, we conservatively estimate that ~20% of ions (in the parent ion distribution) exhibit a significant level of fragmentation (in the fragment ion distribution). From other work in our laboratory [22] (and work from other groups [32]) it is clear other ions can be broken apart by using different ion-neutral collision conditions (another recent approach involves the use of surface induced dissociation. For a discussion see Ref. [33]). We are currently developing a data acquisition system that allows the acceleration potential to be varied during the acquisition of $t_D(t_F)$ windows in order to increase the number of different ions that dissociate [34].

Several additional limitations are also apparent with this instrumental prototype. Although we have recently reported ~3 to 17 fmol detection limits for peptides from parent ion $t_D(t_F)$ analyses, and about an order of magnitude higher limits for fragment analyses [22], improvements in the sensitivities of these methods are still required. Significant gains will be obtained by addressing ion transmission through the drift tube and issues associated with losses during the pulse cycles. For example, with respect to the former problem, we have recently improved transmission at the exit of the drift tube (by a factor of ~5 to 10) by incorporating a differentially-pumped orifice skimmer cone region that is designed to focus ions through the exit region of the drift tube [21]. With respect to the latter constraint, the efficiency of accumulating intense ion beams in an ion trap is quite low. For weak beams, the efficiency of ion accumulation approaches the 100% duty factor that can be calculated by considering accumulation and pulse out times [27]. However, space charging limits the efficiency of trapping intense beams. We are currently working on developing other trapping techniques to address this issue [35]. For example, recently Campbell et al. have shown that the trapping capacity of a 20 cm linear quadrupole trap exceeds that of a Paul geometry trap by almost an order of magnitude [36].

We are also addressing issues associated with efficient ion injection (into the drift tube) as well as resolution of the mobility instrument. We note that the injected ion configuration is intrinsically a low-resolution IMS configuration [28]. Significantly higher resolving powers are attainable with high-pressure drift tubes [37–39], and recently fragmentation at the exit of a high-pressure instrument has been reported [40]. The advantages associated with the very fast gas-phase separation, combined with the idea that ions can be dispersed (rather than discarded in a filtering process) to allow collision-induced dissociation to be carried out in a parallel fashion become even more important as mixture complexity increases. We are currently working on applying this technique for the urinary proteome [41].

Acknowledgements

This work is supported in part by grants from the NIH (1R01GM-59145-02) and NSF (CHE-0078737). We also acknowledge support from the Camille and Henry Dreyfus Foundation. C.S.H.-H. gratefully acknowledges support from an American Chemical Society Division of Analytical Chemistry Graduate Fellowship—sponsored by Merck & Co. C.A.S.B. gratefully acknowledges support from an American Chemical Society summer graduate fellowship from Dow Chemical Company. The authors thank Dr. Katianna Pihakari for help in generating Fig. 2.

References

[1] J.B. Fenn, M. Mann, C.K. Meng, S.F. Wong, C.M. Whitehouse, Science 246 (1989) 64.
[2] M. Karas, F. Hillenkamp, Anal. Chem. 60 (1988) 2299.
[3] B.T. Chait, S.B.H. Kent, Science 257 (1992) 1885.
[4] K. Biemann, Annu. Rev. Biochem. 61 (1992) 997.
[5] K. Biemann, H.A. Scobel, Science 237 (1987) 992;
J.A. Loo, C.G. Edmonds, R.D. Smith, Science 248 (1990) 201;
J.A. Loo, C.G. Edmonds, R.D. Smith, Anal. Chem. 63 (1991) 2488;
S.A. McLuckey, G.J. Van Berkel, G.L. Glish, J. Am. Soc. Mass Spectrom. 3 (1992) 60;
S.A. McLuckey, S.J. Habibgoudarzi, J. Am. Chem. Soc. 115 (1993) 12085;
M.W. Senko, S.C. Beu, F.W. McLafferty, Anal. Chem. 66 (1994) 415;
G. Siuzdak, Proc. Natl. Acad. Sci. USA 91 (1994) 11290;
N.L. Kelleher, H.Y. Lin, G.A. Valaskovic, D.J. Aaserud, E.K. Fridriksson, F.W. McLafferty, J. Am. Chem. Soc. 121 (1999) 806;

J.L. Stephenson Jr., S.A. McLuckey, Anal. Chem. 70 (1998) 3533;
G.E. Reid, J. Wu, P.A. Chrisman, J.M. Wells, S.A. McLuckey, Anal. Chem. 73 (2001) 3274.
[6] T. Ideker et al., Science 292 (2001) 929;
M. Jaquinod, T.L. Holtet, M. Etzerodt, I. Clemmensen, H.C. Thogersen, P. Roepstorff, Biol. Chem. 380 (1999) 1307;
M. Roos, V. Soskic, S. Poznanovic, J. Godovac-Zimmermann, J. Biol. Chem. 273 (1998) 924.
[7] J. Ji, A. Charkraborty, M. Geng, X. Zhang, A. Amini, M. Bina, F. Regnier, J. Chromotogr. B 745 (2000) 197;
M. Geng, J. Ji, F.E. Regnier, J. Chromatogr. A 870 (2000) 295;
S.P. Gygi, B. Rist, S.A. Gerber, F. Turecek, M.H. Gelb, R. Aebersold, Nat. Biotechnol. 17 (1999) 994;
P. Dais, W. Staudenmann, M. Quadroni, C. Korostensky, G. Gonnet, M. Kertesz, P. James, Electrophoresis 18 (1997) 432.
[8] M.R. Wilkins, Biotechnol. 14 (1996) 61;
M.R. Wilkins, K.L. Williams, R.D. Appel, D.F. Hochstasser, Proteome Research: New Frontiers in Functional Genomics, Springer Verlag, Berlin, 1997;
A. Pandey, M. Mann, Nature 405 (2000) 837.
[9] D. Wittmer, Y.H. Chen, B.K. Luckenbill, H.H. Hill, Anal. Chem. 66 (1994) 2348.
[10] D.E. Clemmer, R.R. Hudgins, M.F. Jarrold, J. Am. Chem. Soc. 117 (1995) 10141.
[11] G. von Helden, T. Wyttenbach, M.T. Bowers, Science 267 (1995) 1483.
[12] S.C. Henderson, S.J. Valentine, A.E. Counterman, D.E. Clemmer, Anal. Chem. 71 (1999) 291.
[13] S.J. Valentine, A.E. Counterman, C.S. Hoaglund, J.P. Reilly, D.E. Clemmer, J. Am. Soc. Mass Spectrom. 9 (1998) 1213.
[14] S.J. Valentine, A.E. Counterman, C.S. Hoaglund-Hyzer, D.E. Clemmer, J. Phys. Chem. 103 (1999) 1203.
[15] C.A. Srebalus, J. Li, W.S. Marshall, D.E. Clemmer, Anal. Chem. 71 (1999) 3918.
[16] S.J. Valentine, A.E. Connterman, D.E. Clemmer, J. Am. Soc. Mass Spectrom. 10 (1999) 1188.
[17] Y. Liu, D.E. Clemmer, Anal. Chem. 69 (1997) 2504.
[18] C.S. Hoaglund, Y. Liu, M. Pagel, A.D. Ellington, D.E. Clemmer, J. Am. Chem. Soc. 119 (1997) 9051.
[19] A.E. Counterman, A.E. Hilderbrand, C.A. Srebalus Barnes, D.E. Clemmer, J. Am. Soc. Mass Spectrom. 12 (2001) 1020.
[20] C.S. Hoaglund-Hyzer, J. Li, D.E. Clemmer, Anal. Chem. 72 (2000) 2737.
[21] Y.J. Lee, C.S. Hoaglund-Hyzer, J.A. Taraszka, G.A. Zientara, A.E. Counterman, D.E. Clemmer, Anal. Chem. 73 (2001) 3549.
[22] C.S. Hoaglund-Hyzer, Y.J. Lee, A.E. Counterman, D.E. Clemmer, Anal. Chem. 74 (2002) 992.
[23] S.J. Valentine, M. Kulchania, C.A. Srebalus Barnes, D.E. Clemmer, Int. J. Mass Spectrom. 212 (2001) 97.
[24] C.A. Srebalus Barnes, A.E. Hilderbrand, S.J. Valentine, D.E. Clemmer, Anal. Chem. 74 (2002) 26.
[25] L.M. Matz, H.M. Dion, H.H. Hill Jr., J. Chromatogr. A 946 (2002) 59.
[26] D.F. Hagen, Anal. Chem. 51 (1979) 870;
H.H. Hill, W.F. Siems, R.H. St. Louis, D.G. McMinn, Anal. Chem. 62 (1990) 1201A.
[27] C.S. Hoaglund, S.J. Valentine, D.E. Clemmer, Anal. Chem. 69 (1997) 4156;
S.M. Michael, B.M. Chien, D.M. Lubman, Rev. Sci. Instrum. 63 (1992) 4247;
M.G. Quian, D.M. Lubman, Anal. Chem. 67 (1995) 234A.
[28] D.E. Clemmer, M.F. Jarrold, J. Mass Spectrom. 32 (1997) 577.
[29] C.S. Hoaglund-Hyzer, D.E. Clemmer, Anal. Chem. 73 (2001) 177.
[30] C.S. Hoaglund, S.J. Valentine, C.R. Sporleder, J.P. Reilly, D.E. Clemmer, Anal. Chem. 70 (1998) 2236.
[31] MS Product of Protein Prospector (http://prospector.ucsf.edu/).
[32] A.R. Dongre, A. Somogyi, V.H. Wysocki, J. Mass Spectrom. 31 (1996) 339.
[33] E. Stone, K.J. Gillig, B. Ruotolo, K. Fuhrer, M. Gonin, A. Schultz, D.H. Russell, Anal. Chem. 73 (2001) 2233.
[34] S.J. Valentine, Y.J. Lee, D.E. Clemmer, work in progress.
[35] S. Myung, Y.J. Lee, S.J. Valentine, D.E. Clemmer, work in progress.
[36] J.M. Campbell, B.A. Collins, D.J. Douglas, Rapid Commun. Mass Spectrom. 12 (1998) 1463.
[37] P. Dugourd, R.R. Hudgins, D.E. Clemmer, M.F. Jarrold, Rev. Sci. Instrum. 119 (1997) 2240.
[38] C. Wu, W.F. Siems, G.R. Asbury, H.H. Hill, Anal. Chem. 70 (1998) 4929.
[39] A.E. Counterman, S.J. Valentine, C.A. Srebalus, S.C. Henderson, C.S. Hoaglund, D.E. Clemmer, J. Am. Soc. Mass Spectrom. 9 (1998) 743;
C.A. Srebalus, J. Li, W.S. Marshall, D.E. Clemmer, Anal. Chem. 71 (1998) 3918.
[40] W.E. Steiner, B.H. Clowers, K. Fuhrer, M. Gonin, L.M. Matz, W.F. Siems, A.J. Schultz, H.H. Hill Jr., Rapid. Commun. Mass Spectrom. 15 (2001) 2221.
[41] Y.J. Lee, S.W. Kwon, S. Myung, D.E. Clemmer, work in progress.